

Configuration Effects on Electrode Processes : Optically Active Complexes of Quadridentate Schiff Bases. Part 2.† Iron Complexes

By A. Puxeddu and G. Costa,* Institute of Chemistry, University of Trieste, Italy

Diastereoisomeric chelate complexes of the type $[\text{FeL}(\text{N}_3)]$ (L = a quadridentate Schiff base derived from 1,2-disubstituted ethylenediamine and salicylaldehyde) show differences in several aspects of their electrode behaviour, including the parameters for heterogeneous electron transfer, adsorption on the electrode, and the equilibrium constant of axial-ligand dissociation coupled with the electrochemical reduction.

TRANSITION-METAL COMPLEXES of quadridentate chelating agents having extended π delocalization are useful models of the active site of coenzyme B_{12} , and of oxygen-carrying and electron-transporting biological systems. The polarography of several complexes of the above type was reported in previous papers.¹⁻³ The relation between the characteristics of the electrode processes and the stability and reactivity of the different oxidation states was discussed in terms of electronic effects of the conjugate ligand system. Thus, electronic *trans* (between axial ligands) and *cis* effects (between axial and equatorial

ligands) were demonstrated by the axial co-ordination equilibria,⁴ the rates of nucleophilic reactions of cobalt(I) chelate complexes,^{5,6} and the electrophilic reactivity of cobalt(III) chelate complexes such as the cleavage of a cobalt-carbon bond.^{7,8} All these effects were rationalized by correlation with redox potentials between Co^{III} , Co^{II} , and Co^{I} .^{9,10}

These results prompted us to extend the investigation to the effects of conformation on redox properties and on related chemical behaviour. Suitable model systems related to the previously studied complexes are offered

† Part I is ref. 17.

¹ G. Costa, G. Mestroni, A. Puxeddu, and E. Reisenhofer, *J. Chem. Soc. (A)*, 1970, 2870.

² G. Costa, A. Puxeddu, and E. Reisenhofer, *J.C.S. Dalton*, 1972, 1519.

³ G. Costa, A. Puxeddu, and E. Reisenhofer, *Chem. Comm.*, 1971, 993.

⁴ G. Costa, A. Puxeddu, and E. Reisenhofer, *Coll. Czech. hem. Comm.*, 1971, **36**, 1065.

⁵ G. Costa, A. Puxeddu, and E. Reisenhofer, *Tetrahedron Letters*, 1972, **22**, 2167.

⁶ G. Costa, A. Puxeddu, and E. Reisenhofer, *J.C.S. Dalton*, 1973, 2034.

⁷ G. Costa, A. Puxeddu, and E. Reisenhofer, *Experientia Suppl.*, 1971, **18**, 235.

⁸ G. Costa, A. Puxeddu, and E. Reisenhofer, *Bioelectrochemistry Bioenergetics*, 1974, **1**, 497.

⁹ G. Costa, *Pure Appl. Chem.*, 1972, **30**, 335.

¹⁰ G. Costa, *Co-ordination Chem. Rev.*, 1972, **8**, 63.

by chelate complexes of Schiff bases obtained by condensation of salicylaldehyde with optically active 1,2-disubstituted ethylenediamines.¹¹⁻¹³ The diastereoisomeric *meso* (*m*) and (+) or (-) forms differ in the orientation (pseudo-axial or -equatorial) of the two substituents on the ethylenediamine bridge. Some of the structures of the cobalt complexes were determined by X-ray diffraction¹⁴⁻¹⁶ (Figure 1). The first results

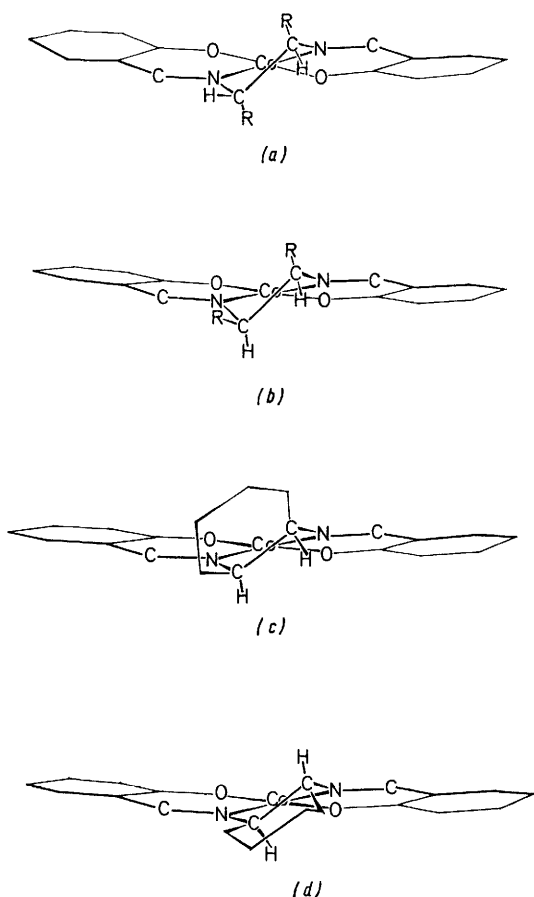


FIGURE 1 Orientation of the substituents on the ethylenediamine bridge: (a) pseudo-bis(axial) in $[\text{Co}\{\text{sal}(\pm)\text{bn}\}]$; (b) and (c) pseudo-axial-pseudo-equatorial in $[\text{Co}\{\text{sal}(m)\text{bn}\}]$ and $[\text{Co}\{\text{sal}(m)\text{chxn}\}]$ respectively; and (d) pseudo-bis(equatorial) in $[\text{Co}\{\text{sal}(m)\text{chxn}\}]$

to demonstrate significant differences in electrochemical behaviour between diastereoisomers were obtained with cobalt(II) derivatives.¹⁷

The present paper deals with iron(III) chelate complexes of general formula $[\text{FeL}(\text{N}_3)]$ and $[\text{FeL}]^+$ (L = a quadridentate Schiff base derived from salicylaldehyde and optically active 1,2-disubstituted ethylenediamine) where the $[\text{N}_3]^-$ ligand is axially co-ordinated with respect to the equatorial chelating agent. The following complexes were examined: $[\text{Fe}(\text{salen})(\text{N}_3)]$ (1) [salen =

NN' -ethylenebis(salicylideneimine)]; $[\text{Fe}\{\text{sal}(+)\text{bn}\}(\text{N}_3)]$ (2), $[\text{Fe}\{\text{sal}(+)\text{bn}\}]^+$ (2a), $[\text{Fe}\{\text{sal}(m)\text{bn}\}(\text{N}_3)]$ (3), and $[\text{Fe}\{\text{sal}(m)\text{bn}\}]^+$ (3a) [salbn = NN' -butane-2,3-diybis(salicylideneimine)]; $[\text{Fe}\{\text{sal}(+)\text{dpen}\}(\text{N}_3)]$ (4) and $[\text{Fe}\{\text{sal}(m)\text{dpen}\}(\text{N}_3)]$ (5) [saldpen = NN' -1,2-diphenylethylenebis(salicylideneimine)]; $[\text{Fe}\{\text{sal}(+)\text{chxn}\}(\text{N}_3)]$ (6) and $[\text{Fe}\{\text{sal}(m)\text{chxn}\}(\text{N}_3)]$ (7) [salchxn = NN' -1,2-cyclohexylenebis(salicylideneimine)].

The evidence for the steric effects is not limited to the characteristics of the electron transfer step, but also includes the dissociation of ligands from the axial positions which are involved in the electrode process and the adsorption of electrochemically active species. The present systems seem to offer one of the very few examples of adsorption of the depolarizer giving rise to a post-wave, instead of the much more frequent pre-wave.

EXPERIMENTAL

Apparatus.—Polarographic measurements were made on an Amel model 471 Multipolarograph equipped with a model 460 Stand. The Multipolarograph includes the electronic circuits and a X-Y recorder. The Stand includes the 'knocker' and the electronic timer to control the dropping time. A model 694 universal cell was used. The characteristics of the dropping mercury electrode (d.m.e.), in dimethylformamide (dmf)-0.1 dm^{-3} $[\text{NET}_4][\text{ClO}_4]$ at 25 °C, were: flow rate = 0.78 mg s^{-1} ; drop time = 3 s; height of the mercury level = 61 cm. A Metrohm saturated calomel electrode (s.c.e.), filled with a saturated aqueous solution of NaCl, was used as the reference electrode. This was separated from the examined solution by means of liquid bridge containing the same supporting electrolyte as in the investigated solution. A platinum ring was used as the counter electrode. Cyclic voltammetry was carried out in the same apparatus.

Controlled-potential electrolysis was carried out with an Amel model 557/SU potentiostat equipped with a self-balancing recorder and a model 563 multipurpose unit, containing the integrator. Experiments were made in a model 693 universal cell with a three-electrode system; a mercury pool of ca. 6 cm^2 was used as the working electrode.

Materials.—Complexes (1)–(7) were a gift from Professor R. Ugo and M. Gullotti. Complexes (2a) and (3a) were obtained as follows. A ca. 1.5 mol dm^{-3} solution (25 cm^3) of (2) or (3) in dmf-0.1 mol dm^{-3} $[\text{NET}_4][\text{ClO}_4]$ was treated with the stoichiometric amount of $\text{Ag}[\text{ClO}_4]$ in dmf; the precipitated $\text{Ag}[\text{N}_3]$ was filtered off. The filtered solution was used directly for the polarographic measurements.

RESULTS

All the polarographic patterns shown by the chelates $[\text{FeL}(\text{N}_3)]$ in the range accessible to the d.m.e. in dmf-0.1 mol dm^{-3} $[\text{NET}_4][\text{ClO}_4]$ are due to one-electron oxidation processes which result in an anodic wave in the range +0.2 to -0.2 V versus the s.c.e. and to two successive one-electron reduction processes which result in three waves in

¹⁴ M. Calligaris, G. Nardin, and L. Randaccio, *J.C.S. Dalton*, 1973, 419.

¹⁵ N. Bresciani, M. Calligaris, G. Nardin, and L. Randaccio, *J.C.S. Dalton*, 1974, 1606.

¹⁶ N. Bresciani, M. Calligaris, G. Nardin, and L. Randaccio, *J.C.S. Dalton*, 1974, 498.

¹⁷ J. Hanzlik, A. Puxeddu, and G. Costa, *J.C.S. Dalton*, 1977, 542.

¹¹ G. V. Panova, E. G. Rukhadze, and A. P. Terent'ev, *Russ. Chem. Rev.*, 1966, **35**, 687.

¹² M. Gullotti, A. Pasini, P. Fantucci, R. Ugo, and R. D. Gillard, *Gazzetta*, 1972, **102**, 855.

¹³ M. Gullotti, C. Casella, A. Pasini, and R. Ugo, *J.C.S. Dalton*, 1972, 339.

the more cathodic region (Figure 2). The anodic process, which is attributed to oxidation of the $[\text{N}_3]^-$ ligand, was not examined further.

The two cathodic waves observed in the range -0.4 to -0.8 V and that in the range -1.7 to -1.9 V (*versus* the s.c.e.) are attributed to changes in the oxidation state of

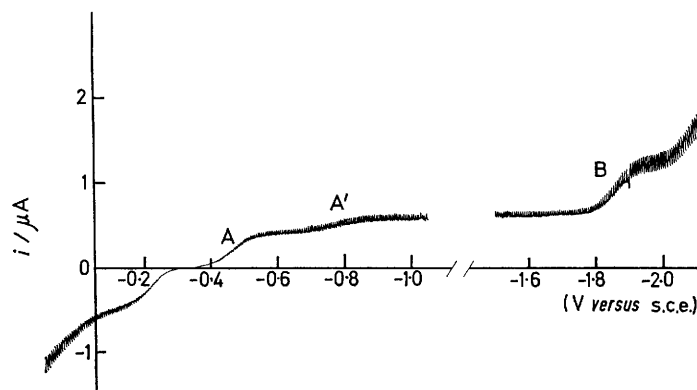


FIGURE 2 Polarographic patterns for $[\text{Fe}\{\text{sal}(m)\text{chxn}\}(\text{N}_3)]$ (0.48×10^{-3} mol dm^{-3}) in $\text{dmf}-0.1$ mol dm^{-3} $[\text{NET}_4][\text{ClO}_4]$ at 25°C

iron, *i.e.* $\text{Fe}^{\text{III}} \rightleftharpoons \text{Fe}^{\text{II}}$ and $\text{Fe}^{\text{II}} \rightleftharpoons \text{Fe}^{\text{I}}$. The first step gives a main wave A followed by a post-wave A'. The second step is the origin of the single wave B at more negative potentials when $[\text{NET}_4][\text{ClO}_4]$ is used as the supporting electrolyte.

The electrode processes are both monoelectronic (see Tables 1 and 2). Thus the diffusion-current constant I is consistent with the value of 1.65 calculated using the diffusion coefficient D from the polarographic limiting currents shown by some cobalt chelate complexes.¹⁷ In 0.1 mol dm^{-3} $\text{Na}[\text{N}_3]$ at 30°C , the logarithmic analysis for the wave A suggests that the electron transfer is reversible (Table 1). The controlled-potential electrolyses give $m = 1$. The reduction products of both process A and B are stable on the time scale of the cyclic voltammetry with a

reversible. The dependence of the current on the square root of the height of the mercury reservoir shows that the process is diffusion controlled (Table 1).

Solutions of $[\text{FeL}]^+$ show a reversible wave A in the range -0.3 to -0.4 V in 0.1 mol dm^{-3} $\text{Na}[\text{ClO}_4]$, at less negative potentials than for the corresponding azide

derivatives in the same supporting electrolyte. The half-wave potential $E_{\frac{1}{2}}(A)$ is shifted by changes in the azide concentration, and the dependence of $E_{\frac{1}{2}}(A)$ on $\log [\text{N}_3^-]$ can be expressed by equation (1), where $(E_{\frac{1}{2}})_c$ is the value of the

$$(E_{\frac{1}{2}})_c - (E_{\frac{1}{2}})_s = 0.059 \log (K_{\text{ox}}/K_{\text{red}}) - (p - q)0.059 \log [\text{N}_3^-] \quad (1)$$

half-wave potential $E_{\frac{1}{2}}(A)$ of $[\text{FeL}(\text{N}_3)]$ at a concentration c of $\text{Na}[\text{N}_3]$ and constant ionic strength made up with $\text{Na}[\text{ClO}_4]$, $(E_{\frac{1}{2}})_s$ is the half-wave potential of the corresponding $[\text{FeL}]^+$ ion at the same ionic strength, $p - q$ is the difference between the number of co-ordinated $[\text{N}_3]^-$ ions in the oxidized and reduced species, and $K_{\text{ox}}/K_{\text{red}}$ is the quotient of the dissociation constants for the $[\text{N}_3]^-$ ligand in the oxidized and reduced chelate complexes. A plot of

TABLE 1
Polarographic characteristics of wave A in $\text{dmf}-0.1$ mol dm^{-3} $\text{Na}[\text{N}_3]$ at 30°C

Complex	$10^3 c$ mol dm^{-3}	$E_{\frac{1}{2}}$ V	$\Delta E / \Delta \log [i/(i_d - i)]$ mV	$\Delta \log i / \Delta \log h$	i_d $\text{cm}^3 \text{t}^{\frac{1}{2}}$
(1)	0.57	-0.622	59		
(2)	0.34	-0.562	60	0.55	1.90
(3)	0.40	-0.590	60	0.50	1.86
(4)	0.41	-0.577	61	0.46	1.52
(5)	0.39	-0.486	61	0.47	1.50
(6)	0.39	-0.621	61		1.43
(7)	0.41	-0.589	59	0.51	1.63

sweep rate of 200 mV s^{-1} . In the presence of excess of $[\text{N}_3]^-$, controlled-potential reduction of $[\text{FeL}(\text{N}_3)]$ gave the corresponding iron(II) complexes which appear to be stable for hours.

First Wave, A—In more concentrated solutions of $[\text{FeL}(\text{N}_3)]$ (1×10^{-3} – 2×10^{-3} mol dm^{-3}) in $\text{dmf}-0.1$ mol dm^{-3} $[\text{NET}_4][\text{ClO}_4]$ or 0.1 mol dm^{-3} $\text{Na}[\text{ClO}_4]$, wave A is more or less irreversible as shown by logarithmic analysis (Table 2) and by the difference between the anodic and cathodic peak potentials measured by cyclic voltammetry. In the case of complex (5), wave A is almost reversible. For all the $[\text{FeL}(\text{N}_3)]$ complexes examined in this concentration range, wave A is diffusion controlled as shown by the linear dependence of the current on the square root of the height of the mercury reservoir. In 0.1 mol dm^{-3} $\text{Na}[\text{N}_3]$ at 30°C at lower concentrations, wave A becomes

$E_{\frac{1}{2}}$ against $\log [\text{N}_3^-]$ (Figure 3) gave $p - q = 1$. Values of $\log K_{\text{ox}}/K_{\text{red}}$ were found to be -5.20 and -5.28 for complexes (2) and (3) respectively.

Second Wave, A'—Dilute solutions (0.1×10^{-3} mol dm^{-3}), in 0.1 mol dm^{-3} $[\text{NET}_4][\text{ClO}_4]$ or 0.1 mol dm^{-3} $\text{Na}[\text{ClO}_4]$, of $[\text{FeL}(\text{N}_3)]$ and $[\text{FeL}]^+$ show only a small wave in the range -0.7 to -0.9 V, *i.e.* the post-wave A'. The height of this wave appears to be dependent on the nature of the supporting electrolyte, and is greater in $\text{Na}[\text{ClO}_4]$ solutions. In more concentrated solutions (10^{-3} mol dm^{-3}), wave A is detectable. On increasing the concentration of the chelate complexes the limiting current of wave A increases, while the limiting current of wave A' becomes constant (Figure 4).

The sum $i_L(A) + i_L(A')$ is proportional to the analytical concentration of the chelate complex. The current has a linear dependence on the height of the mercury reservoir for

wave A' of complexes (3) and (5), suggesting that under these conditions the processes are controlled by adsorption. Although this linear dependence could only be checked for these two complexes which give a relatively higher post-wave hence allowing more accurate measurements, the characteristics of the plot of $i_L(A')$ against concentration confirms that $i_L(A')$ is adsorption controlled in all cases.

DISCUSSION

The electrochemical reduction of the iron(III) chelate complexes takes place in two one-electron steps as was also found for the analogous cobalt species.¹⁷ The two distinct redox steps involve the couples $Fe^{III}-Fe^{II}$ and $Fe^{II}-Fe^I$. The iron(II) species can be obtained by

TABLE 2
Polarographic characteristics of the three waves in dmf-0.1 mol dm⁻³ [NEt₄][ClO₄] [complexes (2)–(7)] or dmf-0.1 mol dm⁻³ Na[ClO₄] [complexes (2a) and (3a)] at 25 °C

Complex	10 ³ c mol dm ⁻³	A			A'	B			A + A'		B
		$E_{1/2}/V$	$\Delta E/\Delta \log [i/(i_d - i)]$ mV	$E_{1/2}/V$		$E_{1/2}/V$	$\Delta E/\Delta \log [i/(i_d - i)]$ mV	i_d cm ² t ^{1/2}			
(2)	1.85	-0.445	87	-0.75	-1.818	70	1.34	1.32			
(3)	1.59	-0.488	70	-0.78	-1.870	73	1.26	1.40			
(4)	2.03	-0.445	91	-0.70	-1.708	63	1.17	1.20			
(5)	1.99	-0.407	59	-0.77	-1.784	81	1.03	1.07			
(6)	2.01	-0.505	81	-0.77	-1.910	72	1.08	1.07			
(7)	1.90	-0.482	70	-0.77	-1.863	68	1.09	1.09			
(2a)	1.38	-0.333	64	-0.73			1.32				
(3a)	1.51	-0.356	62	-0.75			1.33				

The limiting currents of the adsorption waves of the individual chelate complexes at the same complex concentration are different, and a definite difference is also found between the two diastereoisomers of each chelate (Table 3).

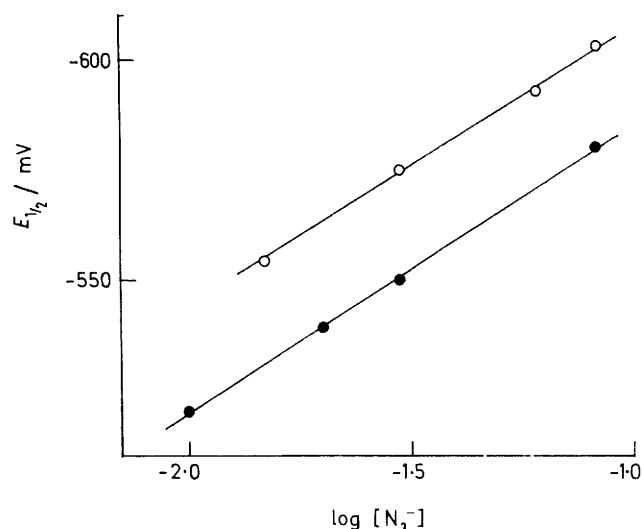


FIGURE 3 Dependence of the half-wave potential of wave A on azide concentration at constant ionic strength in dmf at 25 °C: (○) [Fe{sal(*m*)bn}(N₃)] (0.23 × 10⁻³ mol dm⁻³); (●) [Fe{sal(+)*bn*}(N₃)] (0.21 × 10⁻³ mol dm⁻³)

In the presence of increasing concentrations of [N₃]⁻ at constant complex concentration, $i_L(A')$ decreases (Table 4). In the presence of excess of [N₃]⁻ the adsorption wave is no longer distinguishable.

With the uncharged complexes, $E_{1/2}(A')$ (in 0.1 mol dm⁻³ Na[ClO₄]) shifts to values 200–300 mV more negative than the $E_{1/2}(A)$ value. This displacement is even greater (400 mV) with the corresponding cations of both the diastereoisomers of the salbn derivatives (Table 2).

Third Wave, B.—This wave was observed for all the complexes in dmf-0.1 mol dm⁻³ [NEt₄][ClO₄]. The cationic species [FeL]⁺ were examined using Na[ClO₄] as supporting electrolyte, which limits the accessible potential range to -1.8 V versus the s.c.e. and prevents observation of the process $Fe^{II} \rightarrow Fe^I$.

controlled-potential reduction which occurs with dissociation of the axial ligand only. The iron(I) species, which is also likely to be square planar, is stable on the time scale of cyclic voltammetry. The very negative redox potentials of the $Fe^{II}-Fe^I$ couple suggest that the iron(I) chelates are even more nucleophilic than those of Co^I.

Significant differences, of the same order of magnitude as in the corresponding cobalt complexes, are found between the optically active and *meso* forms of each

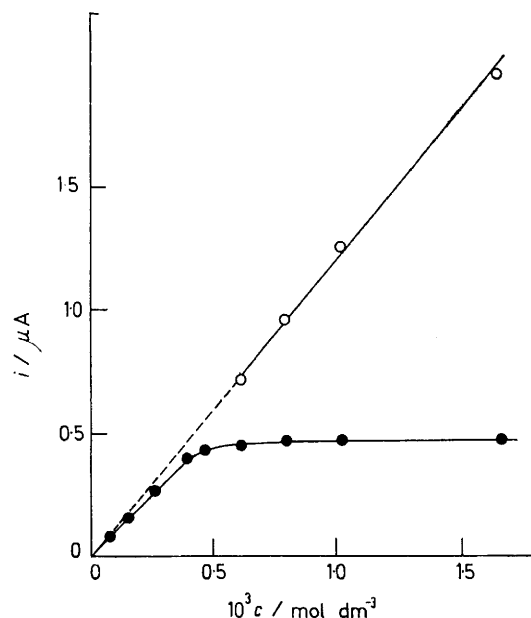


FIGURE 4 Dependence of limiting current on concentration for [Fe{sal(*m*)dpn}(N₃)] in dmf-0.1 mol dm⁻³ Na[ClO₄] at 25 °C (○) $i_L(A) + i_L(A')$; (●) $i_L(A')$

chelate. The differences in $E_{1/2}(B)$ reflect the conformation effects in the reduction of four-co-ordinate iron(II) species. The redox potential of the optically active form is more positive in the salbn and saldpn derivatives, but is less positive in the salchxn derivative. The

situation is the same as in the corresponding four-co-ordinate cobalt(III) complexes,¹⁷ and is consistently related with the stereochemistry if we assume that, as in the cobalt chelates, the conformation is bis(axial) in

TABLE 3

Limiting currents of adsorption waves and the differences $E_{\frac{1}{2}}(A) - E_{\frac{1}{2}}(A')$ at 25 °C

Complex	$i_L/\mu A$		$E_{\frac{1}{2}}(A) - E_{\frac{1}{2}}(A')$ mV
	a	b	
(2)	0.33	0.16	305
(3)	0.70	0.32	292
(4)	0.52	0.31	255
(5)	0.45	0.23	363
(6)		0.18	265
(7)		0.15	288
(2a)	0.17		
(3a)	0.15		

^a In dmf-0.1 mol dm⁻³ Na[ClO₄]. ^b In dmf-0.1 mol dm⁻³ [NET₄][ClO₄].

the optically active salbn and saldpn chelates, axial-equatorial in all the *meso* forms, and bis(equatorial) in the optically active form of the salchxn chelate only.

On the other hand, the relative positions of the $E_{\frac{1}{2}}(A)$

TABLE 4

Polarographic currents of the waves A and A' on increasing azide-ion concentration at 25 °C, [Fe{sal(+)}bn}(N₃) = 0.212 × 10⁻³ mol dm⁻³ in dmf at $I = 0.1$ mol dm⁻³ (Na[ClO₄] + Na[N₃])

$[NaN_3]$ mol dm ⁻³	$E_{\frac{1}{2}}(A)$ V	$\Delta E/\Delta \log [i/(i_d - i)]$ mV	$i_L(A)$	$i_L(A')$ μA	$i_L(A + A')$
0.15	-0.554	66	0.268	0.056	0.324
0.2	-0.567	61	0.278	0.042	0.320
0.3	-0.575	58	0.288	0.022	0.310
0.6	-0.593	62	0.308	0.012	0.320
0.8	-0.603	59	0.320		0.320

values, *i.e.* the reduction potentials of the complexes [FeL(N₃)], reflect the conformation of the five-co-ordinate species. In this series the optically active form is

Co-ord. no.	Stereochemistry		
	Optically active [bis(axial)]	<i>Meso</i> (axial-equatorial)	Optically active [bis(equatorial)]
Four	salbn, saldpn	salbn, saldpn, salchxn	salchxn
Five	salbn	salbn, saldpn, salchxn	saldpn, salchxn

————— Increasingly negative $E_{\frac{1}{2}}$ —————>

reduced at more negative potentials not only in the salchxn but also in the saldpn derivative. The inversion of the position of the redox potentials of the optically active and *meso* forms of the saldpn chelates

in the five-co-ordinate relative to the four-co-ordinate species can be understood if the bis(axial) conformation of the saldpn chelate is switched to bis(equatorial) in the five-co-ordinate species owing to the interactions of the phenyl groups with the axial ligand. It is interesting that the present results are consistent with the patterns of the c.d. spectra where the same trend and inversion was found for the sign of the Cotton effect.¹⁸

The effect of conformation on the redox potentials demonstrates that differences in the distortion of the ligand field around the metal are related to the energy of the frontier molecular orbital in the diastereoisomers. On the other hand, the quotient of the equilibrium constants, K_{ox}/K_{red} , for azide dissociation is about the same in the different conformations. Differences in the free energy of activation for the electron transfer are related to the different flexibility of the molecules of the two diastereoisomers.

The present chelates show an exceptionally neat pattern of adsorption post-wave. The displacement of the half-wave potential of the post-wave relative to the main wave suggests a strong interaction of the depolarizer with the electrode, hindering the electron

transfer. Both the differences $E_{\frac{1}{2}}(A) - E_{\frac{1}{2}}(A')$ and the limiting adsorption current $i_L(A')$ (see Table 3) show the same trend as the half-wave potentials of the main wave A, *i.e.* the sign of the difference between the two five-co-ordinate diastereoisomers in the salbn complexes is opposite to that of both the saldpn and salchxn chelates.

It can be concluded that the present chelate complexes are suitable models for studying the effects of conformation on the interaction of the depolarizer with the electrode, on the chemical equilibria coupled with the redox process, and on the electron transfer itself.

[7/767 Received, 6th May, 1977]

¹⁸ A. Pasini, M. Gullotti, and R. Ugo, *J.C.S. Dalton*, 1977, 346.